Magnetic hyperfine field of isolated Cu impurities in antiferromagnetic Cr metal: experiment and theory

2008 J. Phys.: Condens. Matter 20 015214

(http://iopscience.iop.org/0953-8984/20/1/015214)

J. Phys.: Condens. Matter **20** (2008) 015214 (6pp) doi:10.1088/0953-8984/20/01/015214

Magnetic hyperfine field of isolated Cu impurities in antiferromagnetic Cr metal: experiment and theory

S K Srivastava[1] **and S N Mishra**[2]

[1] Department of Physics and Meteorology, Indian Institute of Technology, Kharagpur-721302, India
[2] Department of Nuclear and Atomic Physics, Tata Institute of Fundamental Research, Homi Bhabha Road, Mumbai-400005, India

E-mail: mishra@tifr.res.in

Received 30 August 2007, in final form 13 November 2007
Published 7 December 2007
Online at stacks.iop.org/JPhysCM/20/015214

Abstract

We report experimental and theoretical studies on the magnetic moment and hyperfine field of Cu impurity in an antiferromagnetic Cr host. Employing time-differential perturbed angular distribution (TDPAD) spectroscopy, the saturation hyperfine field, $B_{hf}(0)$, of ^{62}Cu has been found to be -4.2 T. From the temperature dependence of the hyperfine field measured in the range 35–350 K we find an indication of paramagnetic short-range spin correlation revealed by the observation of a large B_{hf} above T_N. Our *ab initio* calculations using density functional theory (DFT) show a small induced magnetic moment of $\approx 0.18\ \mu_B$ and a net hyperfine field of -7.4 T at the Cu site. The theoretical B_{hf} value agrees with the experimental observation when scaled by the ratio $R = \mu_{Cr}(\text{exp})/\mu_{Cr}(\text{calc})$ between the measured and calculated magnetic moments of Cr.

1. Introduction

Investigations of the magnetic hyperfine field, B_{hf}, for different probes in ferromagnetic and antiferromagnetic materials, which provides microscopic information on magnetic interactions in solids, continues to be an important branch of experimental and theoretical research. Experimentally, over the past decades, extensive measurements have been performed for many different probe nuclei in elemental ferromagnets, e.g. Fe, Co, Ni, and Gd. In general, the magnitude of B_{hf} has been found to scale with the host magnetic moment, μ, showing a simple relation: $B_{hf} = A\mu$, where A is the probe-dependent hyperfine field constant. In comparison, only a few measurements have been made in antiferromagnetic materials. As such, a similar correlation between the hyperfine field and the magnetic moment has not been established in antiferromagnets. In this regard, it is desirable to measure the magnetic hyperfine field for a wider variety of probes in simple antiferromagnets, e.g. Cr.

Chromium is one of the most interesting elements of the periodic table because of its unique magnetic properties [1]. It shows incommensurate spin-density wave (SDW) antiferromagnetic behaviour with $T_N = 311$ K, and undergoes an order–order transformation at 123 K due to a changeover in the orientation of the spins. The magnetism and SDW behaviour of Cr has been studied using hyperfine interaction techniques like Mössbauer spectroscopy (MS) [2] and time-differential perturbed angular correlation (TDPAC) [3]. However, measurements have been limited to only a few probes, e.g. ^{57}Fe, ^{119}Sn, ^{111}Cd, ^{99}Ru, ^{100}Rh and ^{181}Ta [4], mainly due to the unavailability of a larger number of suitable MS/TDPAC probes and metallurgical problems, e.g. the low solubility of relevant impurities in Cr. These experimental difficulties can be overcome by the application of an γ-ray perturbed angular distribution technique (TDPAD) where a wider variety of nuclear probes can be produced via a heavy-ion fusion reaction. Furthermore, the probes thus produced, because of their high kinetic energy, get implanted at depths >1 μm inside the host material, kept immediately behind the reaction target. The method thus allows an elegant way of studying the hyperfine field of extremely dilute (<1 ppm) impurities in different materials, including non-alloying hosts [5, 6].

In this paper, we present the magnetic hyperfine field of isolated Cu impurities in an antiferromagnetic Cr host studied by TDPAD measurements and *ab initio* calculations

within density functional theory (DFT). The experimental measurements carried out using ^{62}Cu as a nuclear probe for the detection of the magnetic hyperfine interaction reveal a saturation hyperfine field $B_{\rm hf}(0) = -4.2$ T. The observed hyperfine field of Cu in Cr, varying weakly with temperature, does not vanish at $T_{\rm N}$ but persists beyond 350 K, suggesting the presence of strong *short-range* spin correlation in the paramagnetic phase. From DFT calculations, we find a small magnetic moment of 0.18 $\mu_{\rm B}$ and a total hyperfine field of $B_{\rm hf}^{\rm tot} = -7.4$ T at the Cu site. The calculated $B_{\rm hf}$ agrees with the experimental value when scaled by the ratio between the measured and calculated magnetic moments of Cr.

2. Experiment and calculation details

TDPAD experiments were carried out at the TIFR/BARC 14 UD Pelletron accelerator facility in Mumbai. For the detection of magnetic interaction we have used the 4^+ isomer in ^{62}Cu, with a half-life $T_{1/2} = 11$ ns and a nuclear gyromagnetic ratio $g_N = 0.67$ [7], as the nuclear probe. The ^{62}Cu nuclei were produced via the heavy-ion reaction ^{52}Cr(^{12}C, pn)^{62}Cu by bombarding a 40 MeV pulsed ^{12}C beam onto a disc of commercially available high-purity (99.99%) Cr metal. The ^{62}Cu atoms thus produced get implanted within the thick Cr host with a typical concentration of less than 1 ppm. The lifetime decay spectra for the 349.5 keV γ-ray from the 4^+ isomer in ^{62}Cu were recorded by two high-purity germanium (HpGe) detectors with a time resolution of $\approx$7 ns at 350 keV. The detectors were kept at an angle of $\pm 135^\circ$ with respect to the beam direction. The measurements were performed at different temperatures ranging from 35 to 350 K in an external magnetic field $B_{\rm ext}$ of 1–3 T applied perpendicular to the beam–detector plane.

The γ-ray angular distributions are perturbed by the hyperfine interaction between the nuclear magnetic moment of the isomeric state and the effective magnetic field $B_{\rm eff} = B_{\rm ext} + B_{\rm hf}$, causing Larmor precession of the nuclear spin which results in a time-dependent modulation of the γ-ray intensity for each detector. From the background subtracted normalized counts $N(\theta, t)$ of each detector, the spin rotation spectra $R(t)$, defined as [5, 6]

$$R(t) = \frac{[N(135^\circ, t) - N(-135^\circ, t)]}{[N(135^\circ, t) + N(-135^\circ, t)]} \qquad (1)$$

were constructed. These were fitted by the function [5, 6]

$$R(t) = (-3/4)A_2\, {\rm e}^{-t/\tau_N} \sin(2\omega_L t - \phi) \qquad (2)$$

to extract the amplitude A_2, the Larmor precession frequency ω_L, and the nuclear relaxation time $\tau_{\rm N}$. The hyperfine field $B_{\rm hf}$ at ^{62}Cu nuclei was then calculated from the relation $\hbar\omega_L = g_{\rm N}\mu_{\rm N}B_{\rm eff}$. The phase factor ϕ in equation (2) accounts for any change in the initial orientation of the nuclear spin which can arise due to finite bending of the incoming ^{12}C beam in the applied magnetic field.

Complementary to the TDPAD experiments, we performed *ab initio* calculations within the framework of density functional theory [8, 9] to study the magnetic moment and hyperfine field of the Cu impurity in the Cr matrix. The calculations were performed using the all-electron full-potential linearized augmented plane wave (FP-LAPW) method, as implemented in the WIEN2k package [10–13]. In this method, the unit cell is divided into two regions: (i) non-overlapping muffin-tin spheres of radius $R_{\rm MT}$ around each atom and (ii) the remaining interstitial region. For the wave functions inside the atomic spheres, a linear combination of radial function times spherical harmonics are used, while in the interstitial region a plane wave expansion is used. In our calculations, we have used $R_{\rm MT}$ values of 2.25 au and 2.35 au for Cr and Cu, respectively. The maximum multipolarity, l, for the waves inside the atomic sphere was restricted to $l_{\rm max} = 10$. The wave functions in the interstitial region were expanded in plane waves with a cutoff of $k_{\rm max} = 7.5/R_{\rm MT}^{\rm min} = 3.33$ au^{-1}. The charge density was Fourier expanded up to $G_{\rm max} = 14\ \sqrt{\rm Ryd}$. For the exchange correlation potential, we used the Perdew–Burke–Ernzerhof (PBE) formalism of the generalized gradient approximation (GGA) [14]. Before calculating the magnetic properties of Cu in Cr, a series of calculations were performed for pure Cr to reproduce some of its physical properties, which served as a reference for the case studied here. For the impurity case, we used a cubic supercell consisting of 27 body-centered cubic (bcc) chromium unit cells ($3 \times 3 \times 3$) having 54 atoms: 53 Cr + 1 Cu, representing an alloy of composition $Cu_{0.0185}Cr_{0.9815}$. In such a unit cell there are eight non-equivalent atoms with lattice positions Cr0/Cu (0, 0, 0); Cr1(1/6, 1/6, 1/6), Cr2(1/3, 0, 0), Cr3(1/3, 1/3, 0), Cr4(1/2, 1/6, 1/6), Cr5(1/3, 1/3, 1/3), Cr6(1/2, 1/2, 1/6) and Cr7(1/2, 1/2, 1/2). The labels for Cr atoms are arranged according to their distance from the origin/impurity, with Cr1 being the closest and Cr7 the furthest. Because of the inhomogeneous environment due to the presence of the impurity, the internal forces on the atoms become non-zero,which need to be minimized. This was achieved by allowing the atoms to relax to new positions such that the force reduces to less than 1 mRyd au^{-1}. In order to find the equilibrium lattice parameter of the unit cell, the energy of the supercell was calculated for different volumes and the results were fitted to the Birch–Murnaghan equation of state [13]. All calculations were performed with initial magnetic structure being antiferromagnetic, with Cr moments of atoms 0, 2, 3, 5 taken to be positive and 1, 4, 6 and 7 taken to be negative. For sampling the Brillouin zone, a k-mesh with 35 special k-points in the irreducible zone (IBZ) was used in the case of supercell calculation while, for the bcc structure of pure Cr, a finer mesh with 120 k-points was taken. It must be mentioned here that calculations were also performed using a smaller ($2 \times 2 \times 2$) supercell with 16 atoms per unit cell, which is equivalent to an impurity concentration of $1/16 = 0.0625$. The results, especially for Cu impurity, were found to be slightly different from those obtained for the larger ($3 \times 3 \times 3$) supercell, indicating a strong influence of the impurity–impurity interaction. Later, for discussion and comparison with the low-concentration (<1 ppm) experimental data obtained from our TDPAD measurements, we shall restrict ourselves to results obtained from the $3 \times 3 \times 3$ supercell.

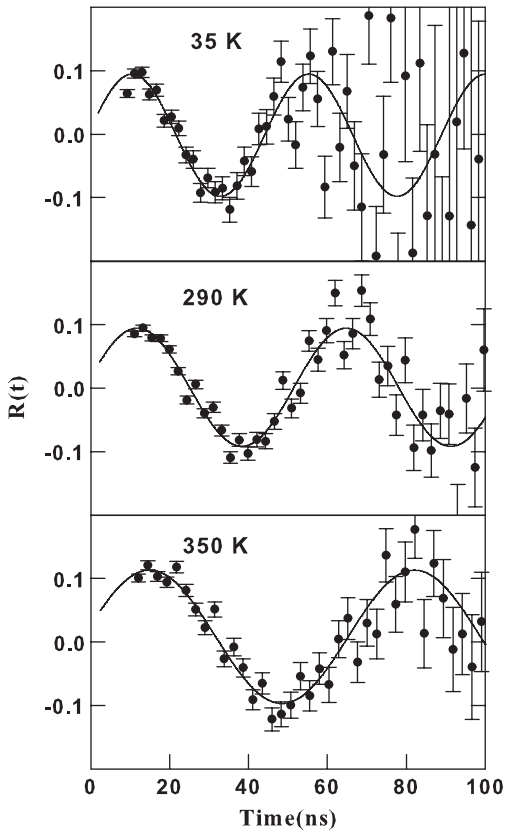

Figure 1. Typical spin rotation spectra of ^{62}Cu in Cr at different temperatures measured in an external magnetic field $B_{ext} = 2$ T. The solid lines are fits to equation (2) (see text) with parameters shown in table 1.

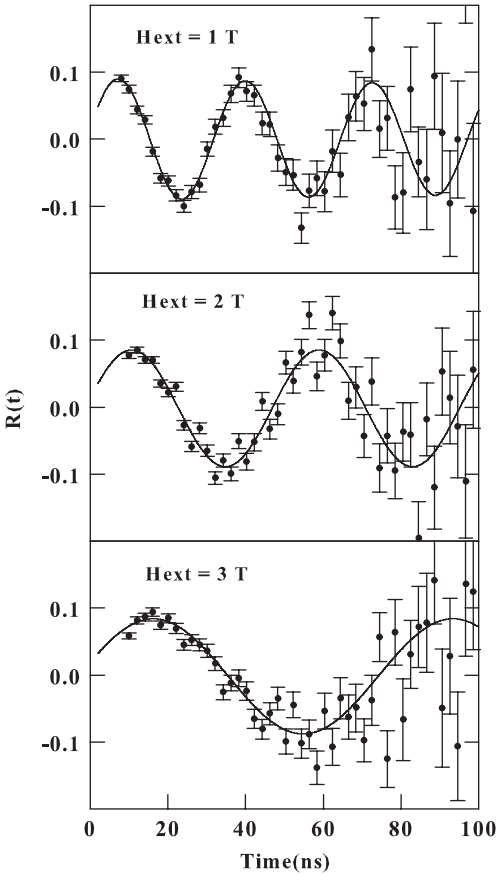

Figure 2. Spin rotation spectra of ^{62}Cu in Cr at 293 K and different applied fields.

3. Results and discussion

Figure 1 shows some typical spin rotation spectra for ^{62}Cu in Cr at different temperatures measured in an external field of 2 T. The spectra measured at all temperatures show a single frequency with high amplitude, $A_2 \approx 0.1$, which indicates that most of the Cu probe atoms produced by the heavy-ion reaction occupy a unique lattice site, most likely to be substitutional. Taking account of the positive sign of the A_2 coefficient [15], the observed sense of rotation in our $R(t)$ spectra implies that the effective field B_{eff} acting on the Cu nuclei is negative. From the observed ω_L, the effective hyperfine field B_{eff} at 35 K was estimated to be -2.2 T, which in turn yielded a hyperfine field $B_{hf} = -4.2$ T. For further confirmation of the sign of the hyperfine field, measurements were also carried out as a function of applied field strength. Figure 2 shows the room-temperature spectra recorded at different external fields. With increasing B_{ext}, ω_L was found to decrease from 108.4 MHz at 1 T to 36.1 MHz at 3 T. The derived B_{eff} as a function of applied field is shown in figure 3 (see inset). It can be seen that B_{eff} decreases linearly with applied field strength, which proves that the hyperfine field of Cu in Cr is indeed negative. The data extrapolated to $B_{ext} = 0$ yielded $B_{hf} = -4.3$ T. Figure 3 displays the variation in B_{hf} as a function of temperature measured at $B_{ext} = 2$ T. With increasing temperature, the B_{hf} value was found to decrease from -4.2 T at 35 K to

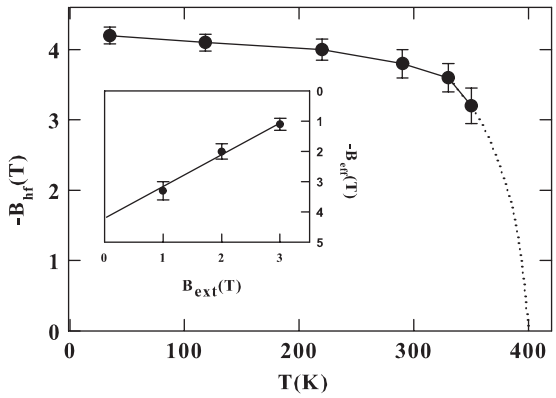

Figure 3. Temperature variation of magnetic hyperfine field B_{hf} for ^{62}Cu in Cr. The dotted line is an extrapolation of the experimental data to $B_{hf} = 0$. The inset shows the variation in the effective field $B_{eff} = B_{hf} + B_{ext}$ seen by the ^{62}Cu probe nuclei at different applied fields.

-3.2 T at 350 K. The hyperfine field results for ^{62}Cu in Cr are summarized in table 1. Extrapolating to $T = 0$, the saturation hyperfine field $B_{hf}(0)$ for Cu in Cr comes out at -4.2 T, which is consistent with the value obtained from external field data. In general, the hyperfine field of a probe nucleus in ferroferromagnetic and antiferromagnetic materials closely follows the temperature dependence of the host magnetization

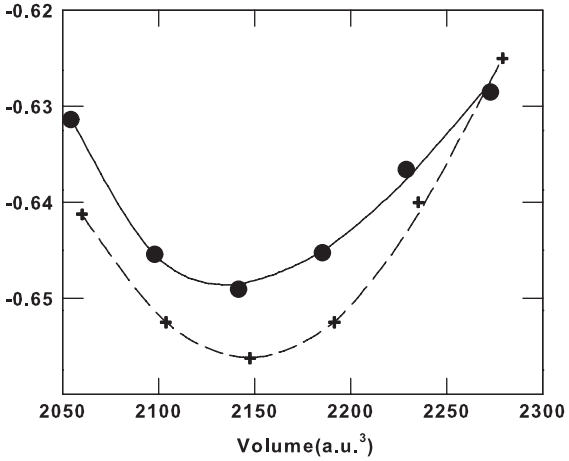

Figure 4. Total energy as a function of unit cell volume for antiferromagnetic Cr (+) and $Cu_{0.0185}Cr_{0.9815}$ alloy (•) corresponding to the $3 \times 3 \times 3$ supercell discussed in the text. The dashed and solid lines are Murnaghan fits.

Table 1. Summary of magnetic hyperfine interaction parameters for ^{62}Cu in Cr measured in an external field of 2 T.

Temp. (K)	A_2	ω_L (Mrad s^{-1})	B_{eff} (T)	B_{hf} (T)
350	0.12(2)	38.5(17)	−1.2(2)	−3.2(2)
330	0.13(2)	48.1(15)	−1.6(2)	−3.6(2)
290	0.10(2)	57.8(14)	−1.8(2)	−3.8(2)
220	0.11(2)	64.2(12)	−2.0(1)	−4.0(2)
118	0.10(2)	67.4(10)	−2.1(1)	−4.1(1)
35	0.11(2)	70.6(9)	−2.2(1)	−4.2(1)

(sublattice magnetization in the case of antiferromagnets) and is expected to vanish just above the ordering temperature T_c (or T_N). In contrast, the $B_{\text{hf}}(T)$ of ^{62}Cu deviates from the temperature dependence of the Cr magnetic moment reported from neutron diffraction measurements [1]. The observed B_{hf} of Cu in Cr, rather than vanishing at $T_N = 311$ K, persists beyond 350 K. The high B_{hf} value observed above T_N suggests an apparent increase in the T_N value, presumably due to strong short-range spin correlations. Our data, extrapolated to $B_{\text{hf}} = 0$, yield a transition temperature of ≈400 K. It is worthwhile mentioning that a similar enhancement of T_N has been reported for thin films of Cr in which the hyperfine field of ^{111}Cd was observed to persist beyond 500 K [16].

It is instructive to compare the hyperfine field results of Cu in antiferromagnetic Cr and a ferromagnetic host like Fe, Co and Ni. The magnetic hyperfine fields of Cu in Fe, Co and Ni have been remeasured to be 17, 13.1 and 4.1 T, respectively [22]. The data are in good agreement with the theoretical estimates made from self-consistent KKR–Greens function calculations [23]. It has been found that the Cu impurity in these ferromagnetic hosts has negligible induced magnetic moment [23–26] and that the hyperfine field arising mainly from the conduction electron polarization (CEP) is linearly proportional to the host magnetic moment: $B_{\text{hf}} = A\mu(\text{host})$ with $A \approx 8$ T/μ_B [22]. Applying this relation to antiferromagnetic Cr with an ordered magnetic moment of 0.62 μ_B [1], the B_{hf} of Cu in Cr is expected to be ≈5 T, which is consistent with our experimental result.

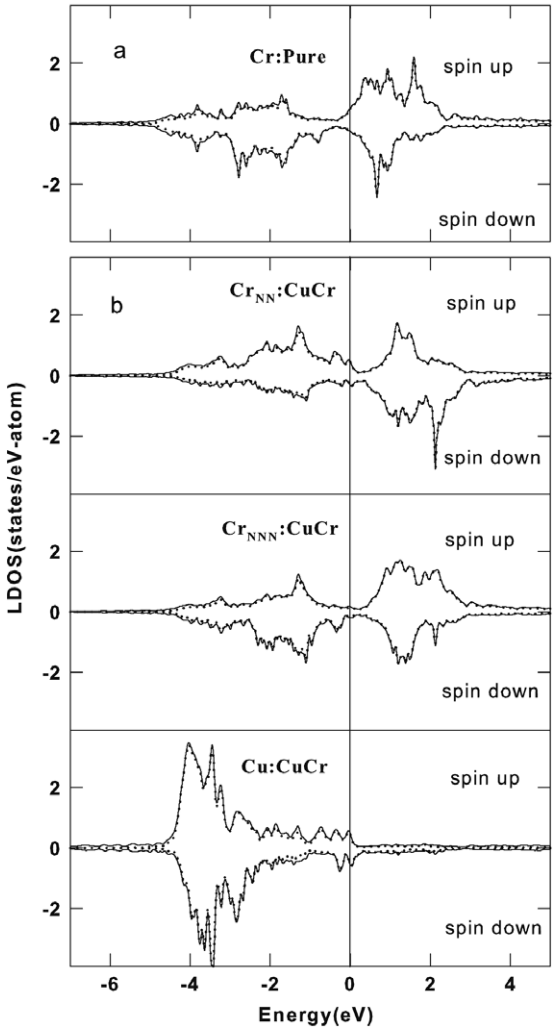

Figure 5. Atom and spin projected density of states (LDOS) of: (a) Cr in pure Cr and (b) Cr and Cu atoms in $Cu_{0.0185}Cr_{0.9815}$ alloy corresponding to the $3 \times 3 \times 3$ supercell (see text). The solid lines are the total DOS while the dotted lines correspond to the d-DOS of the respective atoms.

Coming to the theoretical calculations, figure 4 shows the variation in total energy as a function of unit cell volume for CuCr. The data fitted to Murnaghan equation of state implemented within the WIEN2k program [13] yielded the equilibrium lattice constant of pure Cr as 5.440 au, in agreement with the results reported from earlier calculations [17, 18]. For the CuCr alloy our calculation yielded an equilibrium lattice constant of 5.410 au. Figure 5 shows the spin-resolved density of states (DOS) of pure Cr and CuCr alloy. For pure Cr, our local density of states (LDOS), exhibiting a pseudo-gap structure with Fermi energy E_F located within the gap, are consistent with band structures previously reported in the literature [19–21]. The calculated magnetic moment of Cr at the equilibrium lattice constant comes out to be 1.19 μ_B, in agreement with the results of previous calculations [17, 18]. The calculated magnetic moment, however, is significantly higher than the experimental value [1]. Cottenier *et al* [17] have shown that the magnetic moment of Cr in the antiferromagnetic phase is quite sensitive

Table 2. Summary of calculated properties: supercell lattice constant (a (au)), magnetic moment (μ (μ_B)) and hyperfine fields (B_{hf} (kG)) in pure Cr and CuCr alloy. The numbers within square brackets are the corresponding values obtained from $2 \times 2 \times 2$ supercell calculation.

Host	a	μ		B_{hf}^{tot}	B_{hf}^{core}	B_{hf}^{val}
Cr(Pure)	16.321	1.19		−21.9	−220.3	+198.4
Cu in Cr	16.229	Cr(1nn)	+1.30[1.10]	−34.4[−29.6]	−240.2[−190.0]	+205.8[+160.4]
		Cr(2nn)	−1.20[−1.01]	−5.0[−11.9]	+220.0[+185.6]	−225.0[−197.5]
		Cr(3nn)	−1.17[−0.94]	+21.4[+17.8]	+215.1[+173.3]	−193.7[−155.5]
		Cr(4nn)	+1.19[−0.84]	−20.1[+16.8]	−221.9[+134.0]	+201.8[−117.2]
		Cr(5nn)	−1.16	+12.8	+206.8	−193.9
		Cr(6nn)	+1.15	−3.9	−210.8	+206.9
		Cr(7nn)	+1.14	−8.6	−206.4	+193.9
		Cu(imp)	+0.18[+0.10]	−74.1[−56.3]	−21.4[−10.7]	−52.7[−45.6]

to the exchange correlation potential that was used. While GGA overestimates the magnetic moment with respect to the experimental value, the LDA is unable to find a stable antiferromagnetic (AF) ground state for Cr [19–21]. In the case of CuCr alloy represented by the $3 \times 3 \times 3$ supercell, although the LDOS plots of Cr are qualitatively similar to that of pure Cr, one can see subtle differences, e.g. a slight shift of the d-band closer to E_F. The LDOS of Cu with majority weight coming from the d-band show a small resonance near E_F arising from the hybridization of Cu-d and Cr-d states. For the CuCr alloy, the magnetic moments calculated for the Cu impurity and different near-neighbour Cr atoms are listed in table 2. Looking at table 2, it can be noticed that the Cu atom possesses a small induced magnetic moment of $\approx$0.18 μ_B parallel to the Cr1 moment. In addition, we notice a small perturbation of the Cr magnetic moment. In particular, the Cr atoms closest to the Cu impurity show a slightly higher magnetic moment compared to the value in pure Cr.

Next we turn to the hyperfine field of Cu in Cr. The hyperfine field generally has contributions from dipolar, orbital and Fermi contact interactions. For the case studied here, because of the cubic point symmetry, the orbital and dipolar fields are negligibly small. The dominant contribution to the hyperfine field thus arises from the Fermi contact interaction, which depends on the s-electron spin density at the nucleus $n^s(0)$ and was calculated using the scalar relativistic formula [27] implemented in WIEN2k. The results are shown in table 2. The net hyperfine field of Cu in Cr comes out to be −7.4 T, comprising a sizable core polarization field B_{hf}^{core} of −2.2 T and a valence electron contribution $B_{hf}^{val} = -5.4$ T. The calculated hyperfine field of Cu in Cr turns out to be higher than the experimental value. Since the transferred hyperfine field at the Cu site is proportional to the magnetic moment on the neighbouring Cr atoms, the higher theoretical value of B_{hf} may be due to the larger magnetic moment of Cr predicted from DFT calculations. Recently, Hashemifar *et al* [18] calculated the magnetic moment and hyperfine field of a number of impurities in Cr and found the Cr moment and the impurity hyperfine fields to be higher than the experimental values. However, they found good agreement between the theoretical and experimental B_{hf} values after scaling the valence hyperfine field B_{hf}^{val} by the ratio $R = \mu_{Cr}(\text{exp})/\mu_{Cr}(\text{calc})$ between the measured and calculated magnetic moments of Cr. In general, both B_{hf}^{core} and B_{hf}^{val} are proportional to the magnetic moment μ of the neighbouring magnetic atoms. The scaling law used by Hashemifar therefore is valid only when B_{hf}^{core} is much smaller compared to B_{hf}^{val}. For our case of Cu in Cr, because of the non-negligible core hyperfine field B_{hf}^{core} it is more appropriate to scale the calculated total hyperfine field by the correction factor R. Applying the above argument and using the value of the ordered magnetic moment of Cr, $\mu_{Cr}(\text{exp}) = 0.62\ \mu_B$, reported from neutron diffraction measurements [1], the corrected theoretical hyperfine field of Cu in Cr is estimated to be −3.9 T, which is close to the value obtained from our TDPAD measurements.

4. Conclusion

In conclusion, we have performed experimental and theoretical studies on the magnetic moment and the hyperfine field of Cu impurity in an antiferromagnetic Cr host. From TDPAD measurements using ^{62}Cu nuclei as a probe, the saturation hyperfine field of Cu in Cr has been found to be −4.2 T. As an interesting feature, we find indications of strong short-range spin correlation above the Néel temperature $T_N = 311$ K, reflected by the observation of a large hyperfine field at Cu even at 350 K. Our *ab initio* calculations using density functional theory (DFT) reveal a small induced magnetic moment of $\approx$0.18 μ_B and a net hyperfine field of −7.4 T at the Cu site. The calculated B_{hf} shows good agreement with the experimental results when scaled by the ratio $R = \mu_{Cr}(\text{exp})/\mu_{Cr}(\text{calc})$ between the experimental and theoretical moment values of Cr.

Acknowledgments

We thank S M Davane for his help during the experiment. Support from the Pelletron accelerator facility at the Tata Institute of Fundamental Research (TIFR) is highly appreciated.

References

[1] Fawcett E 1988 *Rev. Mod. Phys.* **60** 209
Fawcett E, Albetrs H L, Galkin V Yu, Noakes R R and Yakhami J V 1994 *Rev. Mod. Phys.* **66** 25
[2] Street R and Window B 1966 *Proc. Phys. Soc. London* **89** 587
[3] Venegas R, Peretto P, Rao G N and Trabut L 1990 *Phys. Rev.* B **21** 3851 and references therein

[4] Rao G N 1985 *Hyperfine Interact.* **24–26** 1119
[5] Mahnke H E 1989 *Hyperfine Interact.* **49** 77
[6] Mishra S N 1994 *Indian J. Pure Appl. Phys.* **32** 602
[7] Raghavan P 1989 *At. Data Nucl. Data Tables* **42** 189
[8] Hohenberg P and Kohn W 1964 *Phys. Rev.* **136** 864
[9] Kohn W and Sham L J 1965 *Phys. Rev.* **140** A1133
[10] Cottenier S 2002 *Density Functional Theory and the Family of (L)APW-methods: A Step-By-Step Introduction* (Belgium: Instituut voor Kern-en Stralingsfysica, K.U.Leuven) ISBN 90-807215-14
[11] Sjöstedt E, Nordström L and Singh D J 2000 *Solid State Commun.* **114** 15
[12] Madsen G K H, Blaha P, Schwarz K, Sjöstedt E and Nordström L 2001 *Phys. Rev.* B **64** 195134
[13] Blaha P, Schwarz K, Madsen G, Kvasnicka D and Luitz J 1999 *WIEN2k: An Augmented Plane Wave+Local Orbitals Programm for Calculating Crystal Properties (Karlheinz Schwarz, Techn. Universitat Wien, Austria)* ISBN 3-9501031-1-2
[14] Perdew J P, Burke K and Ernzerhof M 1996 *Phys. Rev. Lett.* **77** 3865
[15] Chan T U, Agard M, Bruandet J F, Giorni A, Glasser F, Longequeue J P and Morand C 1977 *Nucl. Phys.* A **293** 207
[16] Demuynck S, Meersschaut J, Dekoster J, Swinnen B, Moons R, Vantomme A, Cottenier S and Rots M 1998 *Phys. Rev. Lett.* **81** 2562
[17] Cottenier S, De Vries B, Meersschaut J and Rots M 2002 *J. Phys.: Condens. Matter* **14** 3283
[18] Hashemifar S J, Ghaderi N, Sirousi S and Akbarzadeh H 2006 *Phys. Rev.* B **73** 165111
[19] Chen J, Singh D and Krakauer H 1988 *Phys. Rev.* B **38** 12834
[20] Morruzi V L and Marcus P M 1992 *Phys. Rev.* B **46** 3171
[21] Hafner R, Spisak D, Lorenz R and Hafner J 2002 *Phys. Rev.* B **65** 184432
[22] Lohmann E, Freitag K, Schaefer Th and Vianden R 1993 *Hyperfine Interact.* **77** 103
[23] Akai H, Akai M and Kanamori J 1985 *J. Phys. Soc. Japan* **54** 4257
[24] Zeller R 1987 *J. Phys. F: Met. Phys.* **17** 2123
[25] Drittler B, Stefanou N, Blügel S, Zeller R and Dederichs P H 1989 *Phys. Rev.* B **40** 8203
[26] Paduani C 2004 *J. Magn. Magn. Mater.* **278** 76
[27] Blügel S, Akai H, Zeller R and Dederichs P H 1987 *Phys. Rev.* B **35** 3271